RESEARCH ARTICLE **ISSN 2738-9898 (Print) ISSN 2738-9901 (Online)**

Slope Stability Analysis of Landslide in the Nepalese Himalaya: A Case Study of Kuiyadaha Landslide, Gokuleshor, Baitadi

Sanjay Baral [1*] and Ram Chandra Tiwari [2]

[1] School of Engineering, Faculty of Science and Technology, Pokhara University, Nepal
[2] Pulchowk Campus, Institute of Engineering, Tribhuvan University, Nepal

* Author to whom correspondence should be addressed; E-Mail: *sanjaybaral@pu.edu.np*

Received : 4 November,2024; Received in revised form : 05 December 2024; Accepted : 10 December, 2024; Published: 31 January, 2025

Abstract

Landslides are a common geologic feature in the Nepalese topography. Primary concern of this paper was the numerical modelling along with the case study. This paper describes an investigation into the slope stability of the Kuiyadaha Landslide. The objective of the research is to find out the factor of safety by performing numerical modelling in fully saturation and fully dry condition without vegetation and earthquake loading of creeping landslide of Baitadi District. A back analysis technique was employed to estimate soil strength parameters, where the friction angle (ϕ) was varied, assuming zero cohesion, to achieve a Strength Reduction Factor (SRF) of unity. The derived soil parameters were then utilized to compute the factor of safety (FOS) and recommend stabilization measures, including reducing the groundwater table (GWT) and applying toe loading. Slope stability study was performed using a variety of computational tools, including Cubit, Cygwin, ParaView, Easymesh, AutoCAD, SW DTM, and Tecplot. The SPECFEM3D_GEOTECH software, which uses the Spectral Element Method (SEM), played a crucial role in the analysis. This study discovered that the Kuiyadaha Landslide is extremely prone to slope failure during the rainy season. The stability analysis facilitated the design of effective mitigation measures, highlighting the importance of reduced GWT and toe loading for slope stabilization. Validation of the findings was performed using the Phase2 commercial software. A strong correlation of 0.965 between the results from Phase2 and SPECFEM3D_GEOTECH confirms the reliability of the analysis. This research demonstrates the utility of back analysis and advanced numerical modeling in evaluating and mitigating landslide risks.

Keywords

Landslides, Geotechnical Parameters**,** Numerical modelling, Stability analysis, Back analysis

1. Introduction

In mountainous regions like Nepal, which has fragile geology, slope instability is a common problem. The natural soil in these areas is complex and varies significantly, depending on the characteristics of the parent material and other natural factors. Likewise, natural slopes that have been stable for many years can abruptly fail due to alterations in geometry, external forces, and a decrease in shear strength. Slope failure and landslides are becoming more common in Himalayan regions due to tectonic activities, tectonic stresses and structural planes, earthquake, rainfall or climatic conditions and/or human activities such as civil construction works, deforestation, different agricultural works and many more[1-9]. According to Varnes, there are a number of external or internal reasons that might diminish or enhance shearing resistance [10].

Various studies have been carried out in different periods about slope stability analysis and its risk assessment in mountainous regions. Many researchers have accomplished different numerical techniques for the stability analysis of slope. Limit equilibrium method (LEM), a traditional and well established for the slope analysis, are investigated by the authors[11, 12], modified Fellenius's method and modified Bishop's method to determine the factor of safety of slopes[13]. Bishop method and kinematic analysis are performed to determine the factor of safety[14]. Janbu's generalized procedure of slices (GPS) was applied for the analysis of slope stability[15]. LEM is a common technique for evaluating slope stability by analyzing potential slip surfaces. The slope is divided into vertical slices, and the method calculates the factor of safety (FOS) by ensuring equilibrium of forces and moments for each slice. LEM considers shear strength parameters, pore water pressures, and external loads to determine the likelihood of slope failure. The method is versatile, allowing various assumptions regarding inter-slice forces and different failure mechanisms, making it suitable for diverse geotechnical conditions[16]. These Limit Equilibrium methods have been well-established for many years and remain commonly used in practice due to their simplicity and the relatively reliable results they produce[17].

Finite element analysis (FEM) is a numerical tool used in geology and geotechnical analysis of slopes. Simulation of geometry along with loading, materials, water, and soil behavior are performed in FEM. Under such conditions FEM is used to visualize soil deformations and stress strain behaviors for slope stability and potential failure[16, 18]. The development of FEM was a big solution for slope stability problems. Combination of FEM and LEM eases researcher for the analysis[19]. The FEM not only shows good agreement with factors of safety from limit equilibrium methods but also provides additional performance of slopes as it is based on stress-strain relationship, which traditional methods do not offer [17, 20]. FEM methods are the preferred choice for analyzing slopes stability analysis over LEM[17].

However a high-order finite element method, the spectral element method (SEM) initially appeared in computational fluid dynamics[21]. SEM represents a formulation of FEM in the numerical solution. In seismic wave propagation analysis, researchers have embraced SEM approaches due to its ability to provide minimal numerical dispersion in comparison to current finite element methods. The SEM method adopts the hexahedral elements well, which captures the complexities of the issue domain. It does this by combining the flexibility of FEM with the accuracy of a spectral approach. High-degree Lagrange interpolants are used to discretize the domain of the hexahedral elements, and the Gauss- Lobatto-Legendre (GLL) integration method is used to achieve integration over an element. Combining discretization and integration helps create a simplified mass matrix, which cuts down on computation time and allows for parallel processing, making it the best method for calculating slope instability[4, 22, 23]. In 2012, Gharti and colleagues used the Spectral Element Method (SEM) for the first time to study slope instability within an elasto-plastic framework using the open-source program SPECFEM3D_GEOTECH [24].

The advantage of SEM over existing FEM is SEM utilizes high-order polynomials where integration over an element is performed using nodal quadrature. In this method, the integration and interpolation points align in the nodal quadrature, resulting in a diagonalized mass matrix and eliminating the need for interpolation. Moreover, SEM resolved the issue of distributing interpolation nodes in the tensor-product domain by employing Gauss-Lobatto points. High-order polynomial interpolation ensures the maintenance of both accuracy and efficiency [22].

While many investigations have been conducted on landslides in the Nepalese Himalaya, there is an absence of thorough, site-specific evaluations that combine field data with advanced numerical modeling techniques. Many previous studies provide a broad overview of landslide occurrences and triggers, but they lack precise insights into the mechanics of specific landslides and localized remedies. Despite its tremendous impact, the Kuiyadaha Landslide has not been subjected to a thorough geotechnical examination, resulting in a lack of understanding of its stability conditions and the effectiveness of alternative mitigation techniques. In this study the research question is as follows: What are the primary factors contributing to the instability of the Kuiyadaha Landslide in Gokuleshor, Baitadi, and how can numerical modeling and geotechnical investigations inform effective mitigation strategies? The main objective of this study is to conduct a comprehensive slope stability analysis of the Kuiyadaha Landslide in Gokuleshor, Baitadi, which includes:

1. Conducting detailed field investigations to collect geotechnical data on soil properties, and slope geometry.
2. Utilizing numerical modeling techniques to simulate the slope's behavior under various conditions.
3. Evaluating the effectiveness of potential mitigation measures based on the findings from numerical models and geotechnical data.

By addressing these objectives, this study aims to enhance the understanding of landslide dynamics in the Nepalese Himalaya and contribute to the development of more effective mitigation strategies tailored to the region's unique geological and climatic conditions.

2. Materials and Methods

2.1 Data collection

A site visit was conducted as part of the case study on landslides in Kuiyadaha Village, located in Baitadi District in the Far Western Region of Nepal. The study area map of the site and the sample collection locations are presented in Figure 1 and 2. The purpose of the visits was to collect the necessary survey data, reports if available and soil samples for laboratory investigations.

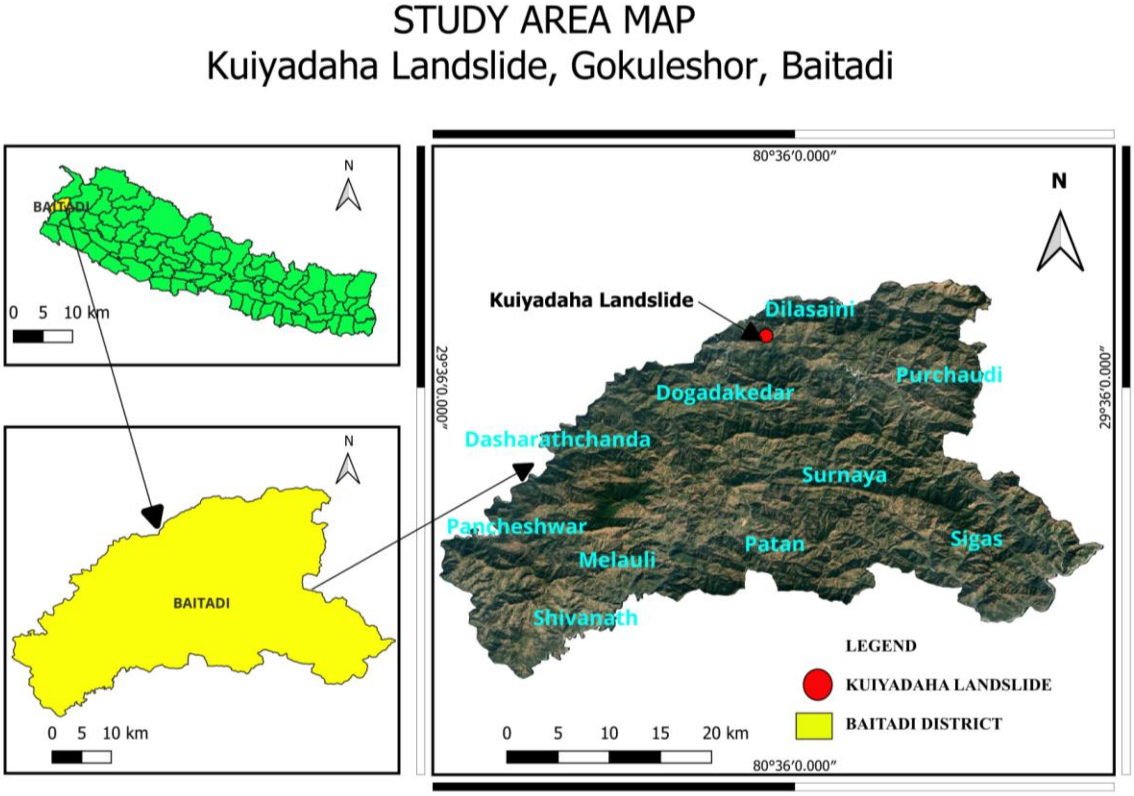

Figure 1: Study Area Map Depicting Kuiyadaha Landslide Location in Gokuleshor, Baitadi District, Nepal

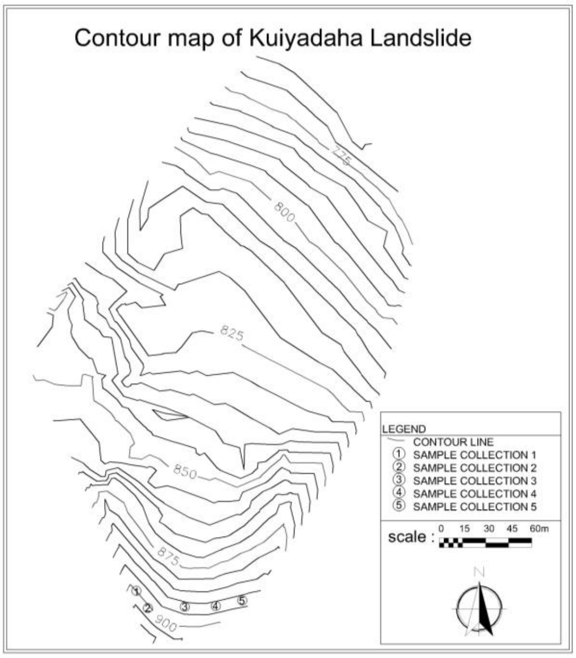

Figure 2: Contour map of Kuiyadaha Landslide

Figure 2 shows a contour map of the landslide area prepared by collecting coordinates of the respective area by performing survey of the area. The site was divided into five sections for the purpose of analysis and accordingly disturbed and undisturbed soil samples were collected from respective sections. Undisturbed samples were collected by using thin-wall tube sampler from open pit sampler method. Various experimental analyses were performed to observe the different characteristics of the soil samples collected from the site, including grain size distribution, liquid limit and plastic limit tests, specific gravity tests, and direct shear tests.

2.2 Grain Size Distribution Test

The grain size distribution test for sieve analysis was done in accordance with ASTM D6913 in order to classify the soil and forecast its behavior [25]. This test helps to understand soil gradation, which is important for engineering applications such as slope stability and foundation design. The results yielded a grain size distribution curve, which provided vital information about the soil's mechanical qualities. Finer grains ($d < 75$ μm) were evaluated using a hydrometer test as per ASTM D7928 [26], which further complemented the categorization procedure. These assessments are critical for assessing soil suitability in the research region and making informed engineering decisions.

2.3 Liquid Limit

The liquid limit (LL) of the soil samples was determined as per the Casagrande method (ASTM D4318) [27]. This parameter is critical for assessing the consistency and shear strength of fine-grained soils, which directly influence slope stability. The liquid limit helps evaluate the soil's susceptibility to deformation and failure under varying moisture conditions, providing essential insights for stability analysis in the study area.

2.4 Plastic limit

The plastic limit (PL), plasticity index (PI), and liquidity index (LI) were determined following standard procedures, such as ASTM D4318 [27], which is commonly used for soil testing. These parameters are essential for assessing the soil's behavior, especially in relation to its plasticity and stability under varying moisture conditions. The plasticity index (PI), calculated by subtracting the plastic limit (PL) from the liquid limit (LL), indicates the moisture content range within which the soil exhibits plastic behavior. For the stability analysis, soil samples were taken from five distinct sections across the study area to account for variations in soil properties. These samples were analyzed to provide a comprehensive understanding of the soil's plasticity characteristics, which are critical for assessing slope stability and designing mitigation measures for potential landslides.

2.5 Grain density test

The grain density of the soil samples was determined using a calibrated pycnometer, following the standard procedure outlined in ASTM D854 for grain density determination. This test is critical for evaluating the physical properties of the soil, which directly impact its behavior under load and moisture variations, both of which are important for slope stability analysis.

2.6 Direct Shear Test

The direct shear test (e.g., ASTM D3080) was conducted to determine the shear strength of the soil samples. This test is particularly useful for evaluating the soil’s behavior under shear forces, which is essential for assessing slope stability and bearing capacity. The direct shear test provides valuable parameters (Figure 3), such as cohesive strength (c) and internal friction angle (ϕ), which are critical for stability analysis. These parameters are derived by plotting normal stress (σ) against shear stress (τ), creating a shear strength envelope. The results are used to understand the soil's shear resistance and its potential for failure under different loading conditions.

For the stability analysis, five distinct soil sections were sampled from the selected locations within the study area. This is crucial for accurate slope stability evaluation and the design of appropriate mitigation measures[28].

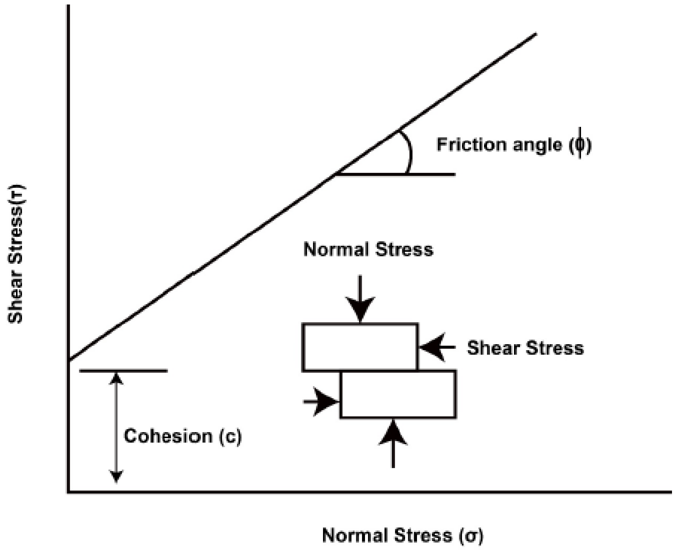

Figure 3: Relationship between Normal stress and Shear stress [29]

2.7 Numerical tools and model

SPECFEM3D_GEOTECH is a free, open-source software that analyzes 3D slope stability and simulates 3D multistage excavation using the spectral-element approach. SPECFEM3D_GEOTECH can be used on single-processor and multi-core systems, as well as huge computing clusters. It is primarily written in FORTRAN 90. This program does not calculate the factor of safety for slope stability. Instead, simulations can run over a variety of safety factors, and graphing the safety factor vs maximum displacement allows the slope's factor of safety to be determined. While SPECFEM3D_GEOTECH is designed for slope stability and multistage excavation assessments, it is also suitable for various quasistatic simulations in solid and geomechanics.

The investigation begins with a thorough desk review of papers about slope failure and landslides. Contour maps of the area are created (Figure 2) and thoroughly researched, with a particular emphasis on the region's geotechnical properties. Fieldwork collects all essential geological and geotechnical data, and a direct shear test is used to estimate soil shear strength values. Slope profiles of the area are prepared using AutoCAD, SW_DTM and are modeled as a 2D plane strain problem. Meshing and mapping operations are conducted in Cubit, with fixed boundaries applied to the bottom, left, and right faces of the models. Numerical analyses are then performed using the Specfem3D_Slope serial program on the Cygwin platform [24]. The results obtained are subsequently analyzed using post-processing tools such as Tackplot and Paraview. Finally, relevant mitigating solutions are provided after validating findings with the finite element method (FEM) program, Rocscience Phase2. The process is shown in Figure 4 below.

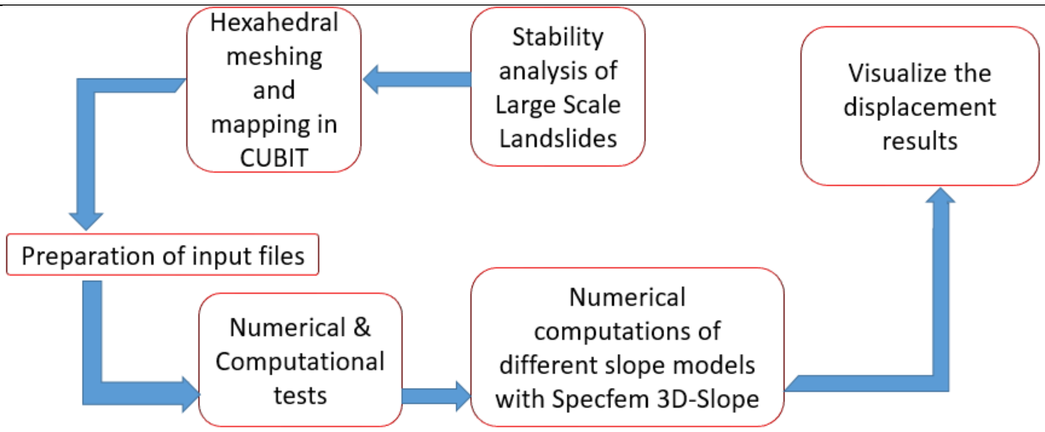

(a)

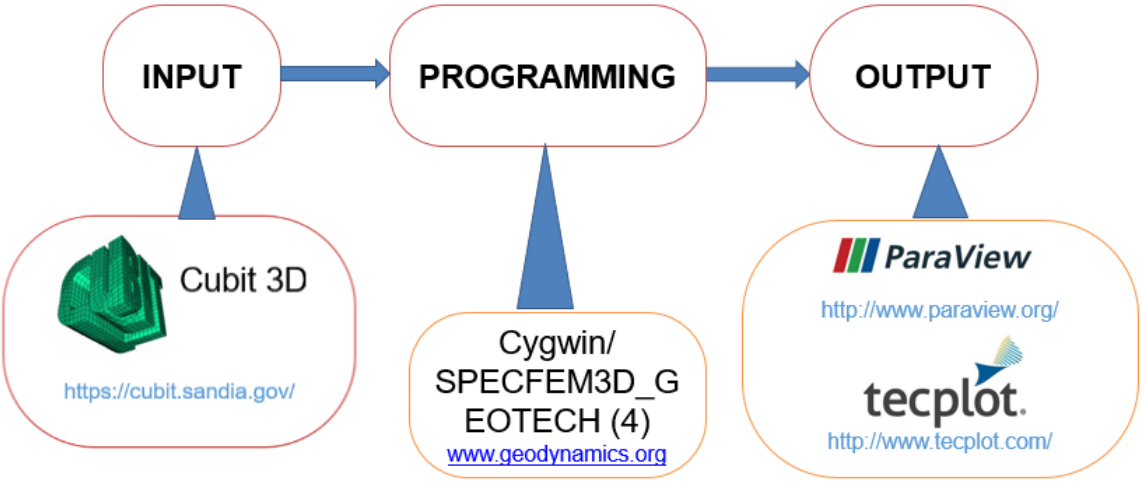

(b)

Figure 4: (a) Numerical procedure and (b) computational procedure

Regarding the slope in critical condition the following type of slope will be considered in modelling:

a. Fully saturated slopes with no vegetation and no earthquake loading.
b. Gradual reduction of the groundwater table (GWT) in intervals of 1 meter, up to a minimum depth of 10 meters, and additional reductions as required.
c. Dry slope with no vegetation and no earthquake loading.
d. Toe loading with varying GWT as stabilizing measures.

2.8 Model Preparation

Creating a realistic model requires accurate topography, ideally obtained through a survey, which captures detailed contours to build both 2D and 3D models. So, through the site visit and detail survey of the Kuiyadaha Landslide a contour map is prepared (Figure 2) selecting appropriate contour intervals. In Cubit or AutoCAD, build the model geometry based on survey-derived contour data. Prepare it to be meshable, then proceed with the meshing process by setting mesh parameters and verifying mesh quality (Figure 5). Once the meshing is complete and quality-checked, apply the necessary boundary conditions to the model. Six soil properties are used to generate the material model: dilation angle (ψ), internal friction angle (ϕ), cohesion coefficient (C), Poisson's ratio (ν), Young's modulus (E), and unit weight (γ). For analytical purposes, these factors describe the mechanical and physical characteristics of the soil [23]. The graph of SRF vs maximum displacement is plotted using Tacplot to display data in two dimensions. The critical factor of safety is then evaluated to determine the factor of safety. The point at which displacement suddenly changes to its maximum is known as the critical value of SRF.

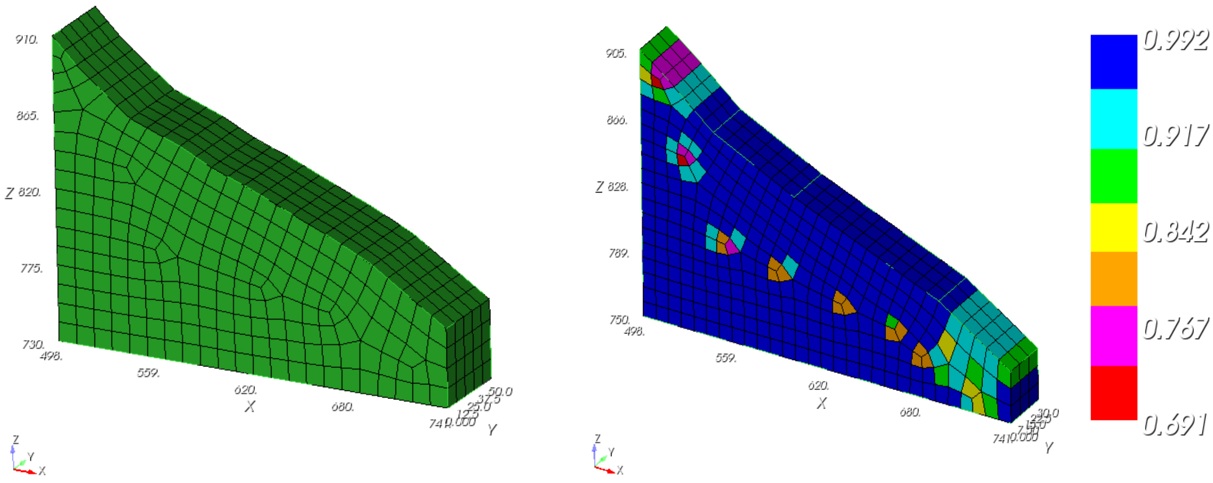

(a) (b)

Figure 5: Typical Kuiyadaha landslide model at Section 3: (a) Geometry in Cubit and Meshing operation in Cubit and (b) Meshing with quality refinement in Cubit

3. Results and Discussions

The case study was taken at the landslide which lies on the left side of the Chameliya River above the Mahakali Highway at Kuiyadaha village, Gokuleshor, Baitadi district. The landslide is creeping failure type is taken. The site is located at 164829 Easting, 3286502 Northing and 910 m altitude at crown, 164962 eastings, 3286846 northings and at 760 m altitude, from side 164925 easting 3286617 northing and at 843 m height to side 164780 m easting 3286718 m northing and at height of 851 m. The average length of Kuiyadaha landslide is 400 m whereas its average breadth is 175 m. The landslide was initiated due to natural causes like continuous heavy rainfall for seven long days damaging seriously 11 houses. This is the case of creep failure as it is moving every year during monsoon season (July to September). Local people came to know about the occurrence of landslides by observing the visible cracks developed in the residential houses and the slight movement of the land (Figure 6).

Figure 6**:** Several field features of the Kuiyadaha landslide (a) and (b) Crown and body of landslide area (c) crack developed near crown (d) tilted toilet and (e) displacement of the landslide

3.1 Geotechnical Result

From the results of direct shear test, the internal friction angle and cohesion of soil samples were determined. The graph (Figure 7) shows a linear relationship between shear stress (on the y-axis) and normal stress (on the x-axis) for the soil samples. The linearity suggests that the soil follows the Mohr-Coulomb failure criterion. From the graph, it appears the lines for different samples intercept the y-axis slightly above 0. The soil samples collected from the Khiyadaha landslide exhibit small but positive cohesion values. This shows the internal friction angle ranges from 15^o-19^o while the cohesion value ranges from 9 kN/m^2 to 12 kN/m^2.

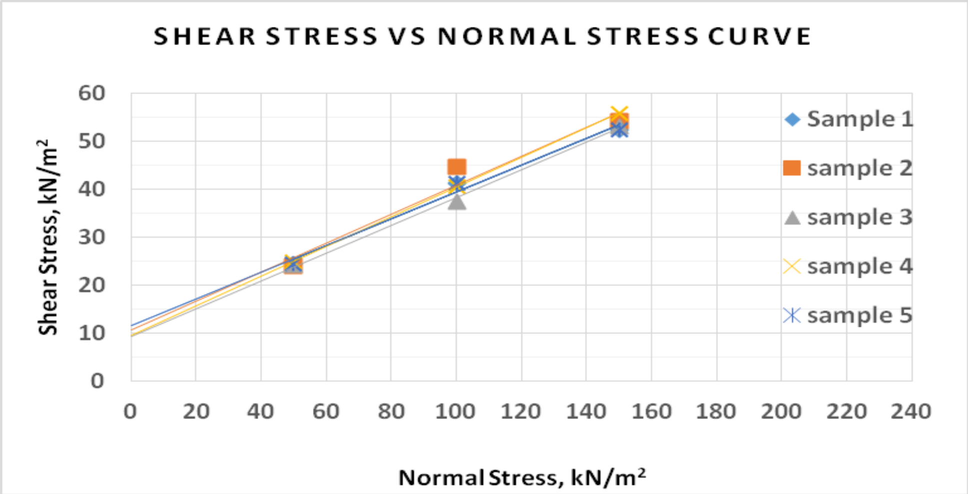

Figure 7: Calculation of shear strength parameters from direct shear test

Table 1: Results of several Geotechnical Parameters

Sample no.		S1	S2	S3	S4	S5
Cohesion c=	KN per sq m	11.45	10.54	9.29	9.41	10.88
Friction angle ϕ=	degree	15.58	16.84	16.12	17.19	18.37
Field Density γ=	gm per cc	1.557	1.726	1.31	1.56	1.61
Grain Size Analysis						
Gravel %		17.9	19.81	49.656	29.655	15.817
Sand %		77.73	78.645	49.225	67.634	81.958
Silt and Clay %		4.37	2.446	1.119	2.711	2.225
Coefficient of Uniformity (C_u)		5.455	5.636	12.267	12.308	8.636
Coefficient of Curvature (C_c)		0.873	0.845	2.806	0.556	0.647
Atterberg Limit						
Liquid Limit (%)		27.200	31.000	35.000	34.250	32.500
Plastic Limit (%)		19.760	13.080	14.320	18.260	17.290
Specific Gravity of soil (G) =		1.925	2.097	2.151	2.025	1.917
Unified Soil Classification System (Class)		SP (Poorly graded Sand)	SP (Poorly graded Sand)	GW (Well graded Gravel)	SP (Poorly graded Sand)	SP (Poorly graded Sand)

The grain size analysis indicates that four samples are classified as poorly graded sand (SP) and one sample as well-graded sand (GW) according to the Unified Soil Classification System (USCS). The grain-size distribution curves for these soils are presented in Figure 8 and summarized in Table 1. The liquid limits of soil samples S1, S2, S4, and S5 range from 27% to 34%, while S3 has a slightly higher liquid limit of 35%. This indicates that S1, S2, S4, and S5 lose their shear strength and transition to a liquid-like state at lower water content compared to sample S3. The unit weights of the materials vary between 1.3 and 1.7 grams per cubic centimeter, with an average value of 1.55 grams per cubic centimeter used for this study.

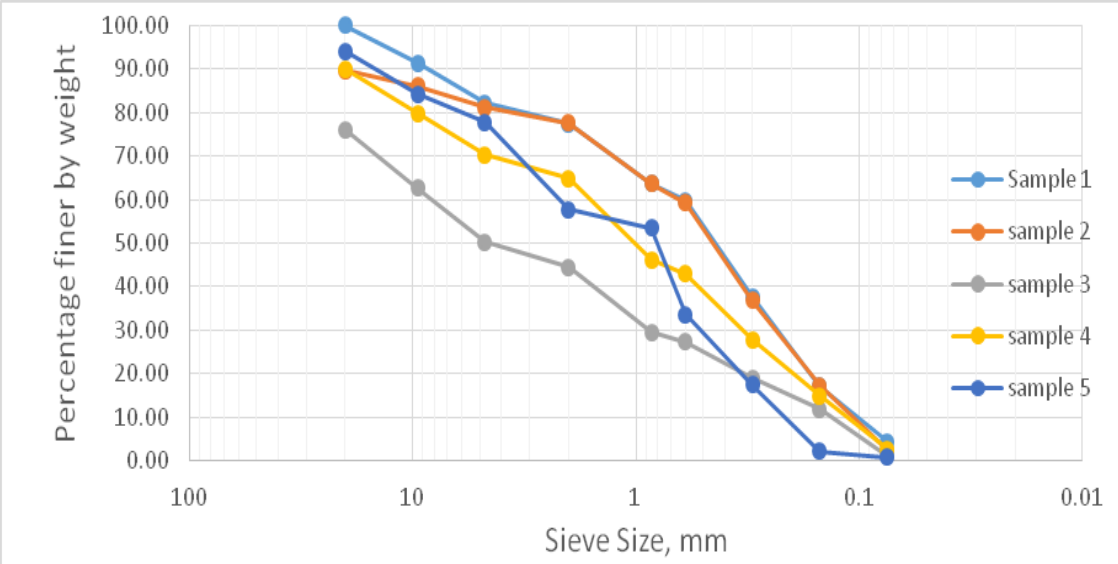

Figure 8: Grain size distribution curves of different soil samples from Kuiyadaha Site

3.2 Back analysis technique

The back analysis technique focuses on evaluating slope stability by considering key soil parameters like cohesion and friction angle. Each parameter is carefully chosen within realistic ranges to avoid implausible combinations [30]. Geotechnical engineers often employ back-analysis to estimate the characteristics of an in-situ rock or soil mass. Slope engineering analysis can predict the minimal operational shear strengths for seemingly stable slopes [31]. Mechanical parameters of soil are typically obtained through laboratory testing on remolded samples. However, due to the complex nature of geological materials, these lab-determined parameters often differ significantly from the actual in-situ values, prompting researchers to focus on determining geotechnical parameters for slopes using numerical back analysis [32-34].

To determine whether the lab test results are accurate, the back analysis (BA) approach is employed, which involves setting the cohesiveness parameter to zero and altering the friction angle. The back analysis approach was performed using the trial-and-error method in SPECFEM3D_GEOTECH by altering the input parameter, i.e. the friction angle, and calculating the corresponding strength reduction factor (SRF). Back and inverse analysis are well-known computational approaches that can give necessary information about unknown factors influencing a studied system or event by employing data provided as output behavior [35]. It is an intermediate problem since there are more unknown than available equations. To simplify the issue and come up with a solution, several presumptions are necessary. The engineering expertise and judgment used to make these assumptions have a significant impact on the results' accuracy which are essential to simplify the problem and make it solvable. Despite its limitations, back analysis can yield practical and reasonably accurate findings when assumptions are carefully validated. This helps to uncover important parameters for slope stability design, such as cohesion and friction angle.

After the slope fails, a representative sample cannot be obtained, hence the laboratory results cannot generate practical shear parameter values. As a result, the BA approach is now recognized as an effective instrument for predicting soil properties. Back analysis is reliable if the model and the assumptions are fair and accurate representations of the actual system. Analysis of slope failure is frequently used to increase one's understanding of slope parameters [35]. By performing the BA technique, the friction angle of the natural slope value of section one and two is 30^0 whereas for section three, four and five is 26^0 27^0 and 28^0 and this is shown in tabular form in Table 2 and Figure 9.

Table 2: FOS values of natural slope for different friction angle (ϕ)

section	S1	S2	S3	S4	S5
ϕ angle					
24		0.8	0.95	0.9	0.88
25		0.85	0.98	0.95	0.92
26	0.7	0.88	1	0.98	0.96
27	0.8	0.9	1.05	1	0.98
28	0.85	0.94	1.1	1.04	1
29	0.9	0.97	1.2	1.1	1.5
30	1	1		1.15	1.2
31	1.05	1.05		1.2	1.25
32	1.1	1.08			
33	1.15				

Comparing the results from lab test and BA technique, the results of BA were found to be more satisfactory than that of lab, it is because of the selected soil sample from the site was after the mass failure (Table 3). Figure 9 illustrates how strength reduction factor (SRF) and maximum displacement vary with changing friction angles (ϕ) for all 5 sections. As the friction angle increases, the slope achieves stability (SRF = 1) at lower displacements. This trend in all 5 sections supports the idea that higher friction angles contribute significantly to slope stability in BA results. The back analysis method, supported by graphical results, proves to be more reliable than lab tests for evaluating slope stability in this study. The discrepancy arises due to lab samples being collected post-failure and the BA's incorporation of real-site conditions. The higher friction angles obtained in BA align with critical slope conditions and validate its use in designing stabilization measures.

Table 3: Comparison of results from lab and BA technique

Section	lab results		BA results	
	cohesion	Friction angle	Cohesion	friction angle
S1	11.45	15.58	0	30
S2	10.54	16.84	0	30
S3	9.29	16.12	0	26
S4	9.41	17.19	0	27
S5	10.88	18.37	0	28

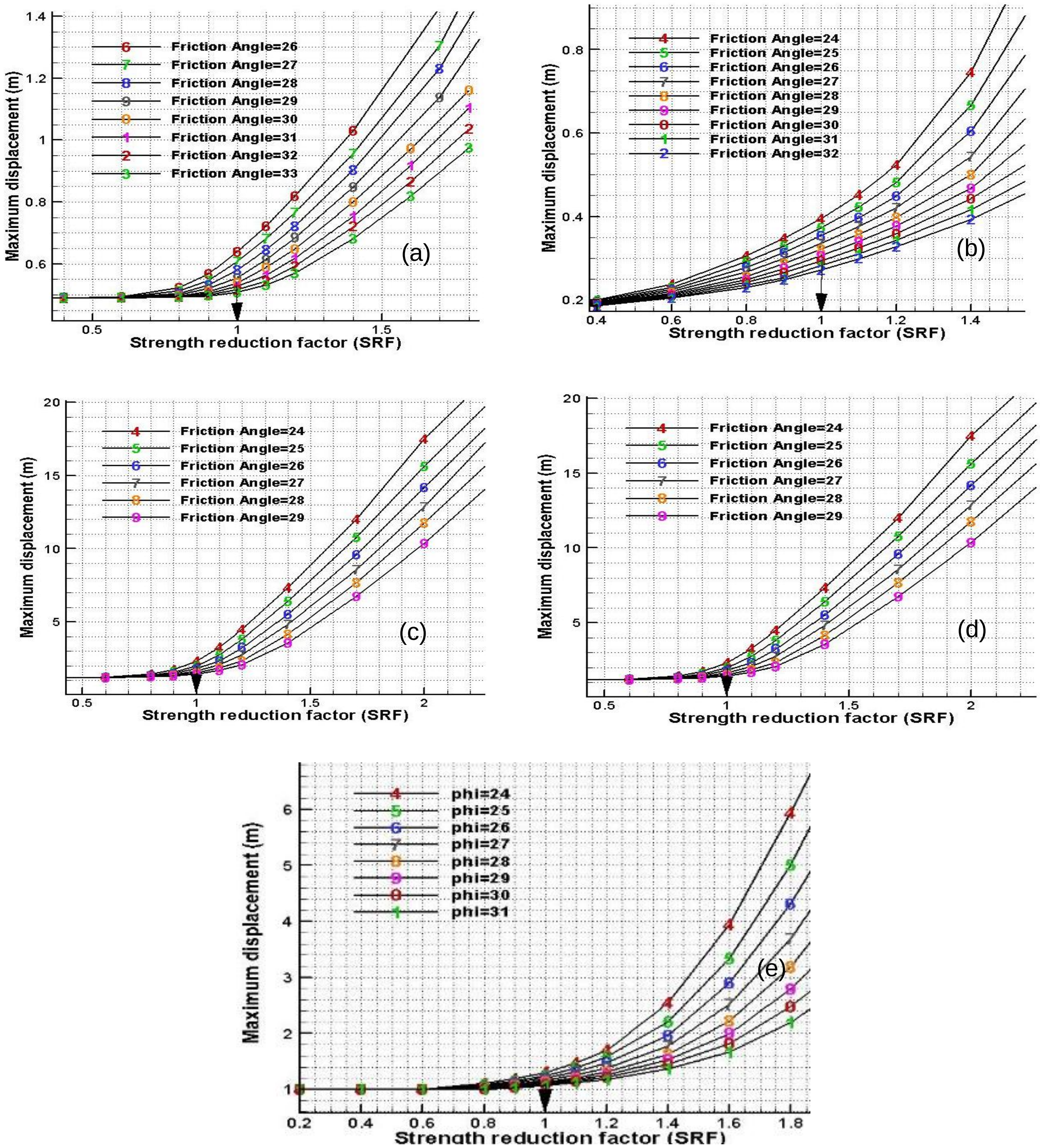

Figure 9: (a) Computational results (back analysis result) of (a) Section 1 (b) Section 2 (c) Section 3 (d) section 4 and (e) Section 5

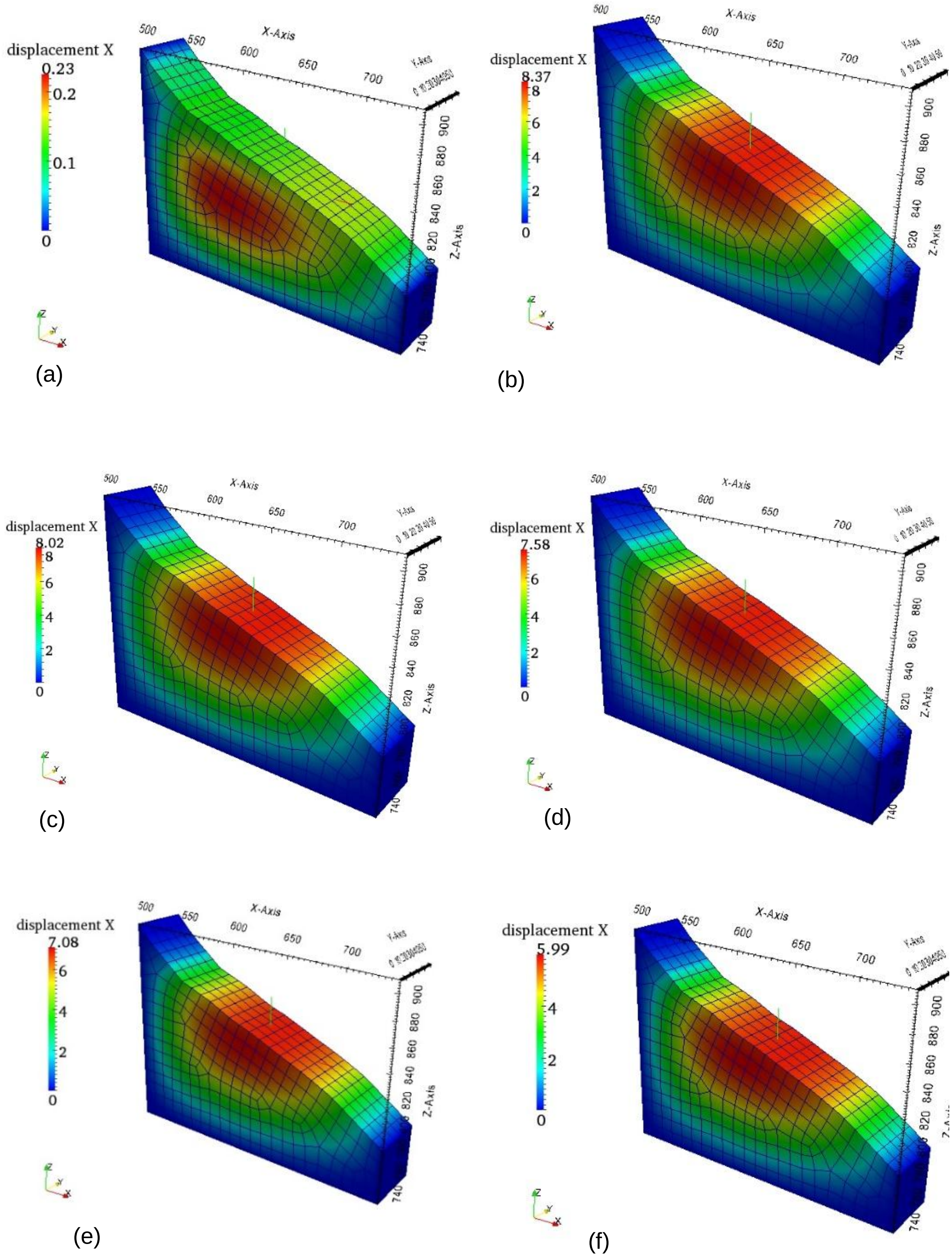

Figure 10: Progressive displacement in varying ground water condition and pore water pressure at section 3 Paraview result (a) Dry condition (b) full saturation condition (GWT at surface) (c) GWT reduction by 2 m (d) GWT reduction by 4 m (e) GWT reduction by 6 m (f) GWT reduction by 10 m

Stability analysis across five sections of the Kuiyadaha slope, with a groundwater table (GWT) lowered by 10 meters, shows varying SRF values, as displayed in Table 4. The slope is most stable in dry conditions and least stable when saturated, indicating failure risk increases with a higher GWT. In Section 1, reducing the GWT by seven meters brings stability equivalent to dry conditions, with further stability possible by lowering the GWT more. Other sections show minor SRF improvements but require additional GWT reduction, potentially over 10 meters, necessitating advanced equipment.

Table 4: FOS for different conditions of natural slope

section	S1	S2	S3	S4	S5
Dry condition	1	1	1	1	1
Saturation condition	0.45	0.4	0.15	0.4	0.4
1 m GWT Down	0.5	0.5	0.2	0.4	0.45
2 m GWT Down	0.6	0.55	0.2	0.46	0.5
3 m GWT Down	0.7	0.58	0.3	0.5	0.52
4 m GWT Down	0.8	0.6	0.35	0.54	0.55
5 m GWT Down	0.85	0.63	0.4	0.56	0.56
6 m GWT Down	0.94	0.7	0.4	0.6	0.58
7 m GWT Down	1	0.76	0.48	0.62	0.62
8 m GWT Down	1.04	0.8	0.5	0.65	0.75
9 m GWT Down	1.15	0.88	0.52	0.68	0.78
10 m GWT Down	1.21	0.9	0.55	0.7	0.8

3.3 Verification of Work

Verification of the work is performed by comparing the result of SPECFEM3D_GEOTECH and using commercial software like PHASE2 which is shown in Table 5.

Table 5: comparison of results from SPECFEM3D_GEOTECH and PHASE2

Tools	SPECFEM3D_GEOTECH	PHASE2
Friction angle	28	29.6
CONDITION	CSRF	CSRF
Full dry case	1	1
Full saturate case	0.27	0.12
1 m WT draw down	0.3	0.28
2 m WT draw down	0.4	0.36
3 m WT draw down	0.45	0.45
4 m WT draw down	0.47	0.5
5 m WT draw down	0.48	0.55
6 m WT draw down	0.52	0.61
7 m WT draw down	0.55	0.66
8 m WT draw down	0.65	0.71
9 m WT draw down	0.7	0.75
10 m WT draw down	0.75	0.78

For the verification of the work, out of five sections, section third was analyzed using Phase2. Both results from SPECFEM3D_GEOTECH and Phase2 are evaluated. The increasing trend in the scatterplot indicates a strong positive correlation between the two approaches. A dotted trend line is presented to demonstrate this association, demonstrating that as CSRF values increase in PHASE2, so do SPECFEM3D_GEOTECH (Figure 11). Correlation is calculated to be 96.5%. Graphs and model of Phase2 are shown in figures 12 and 13.

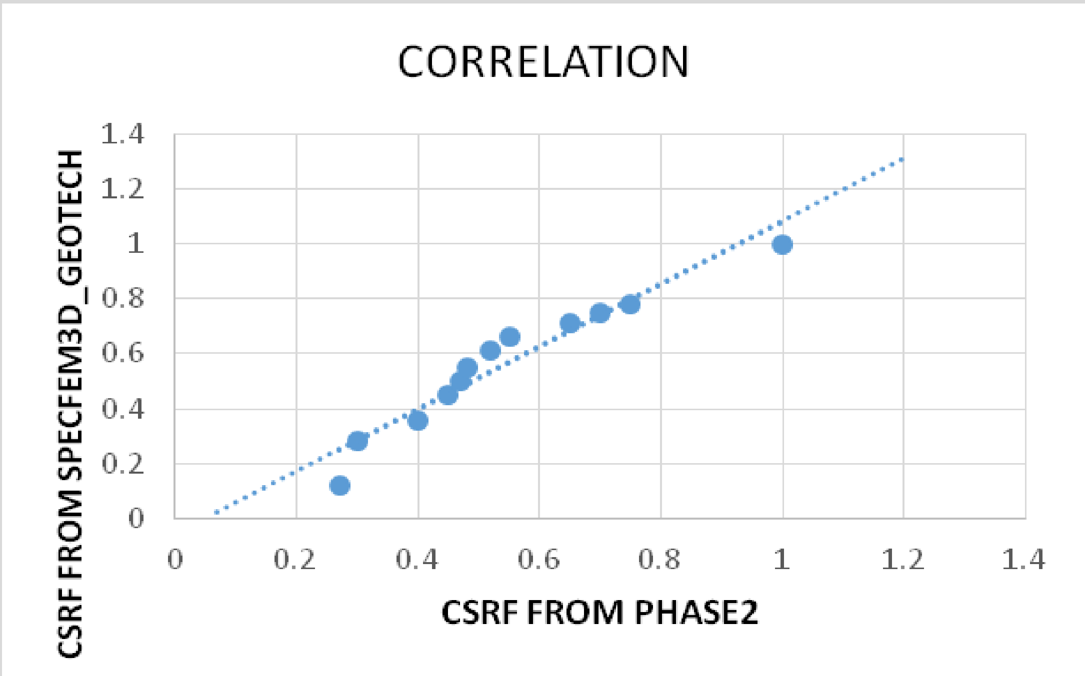

Figure 11: Correlation between the result from SPECFEM3D_GEOTECH and PHASE2 (96.5%)

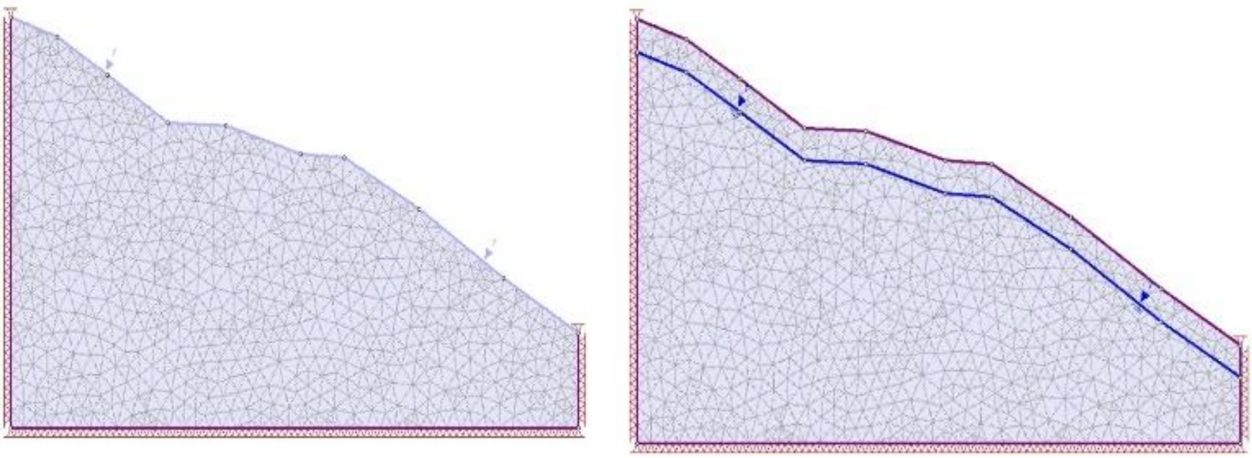

(a) (b)

Figure 12: (a) A phase2 model geometry for full dry condition and (b) A phase2 model geometry for 10m GWT drawdown condition

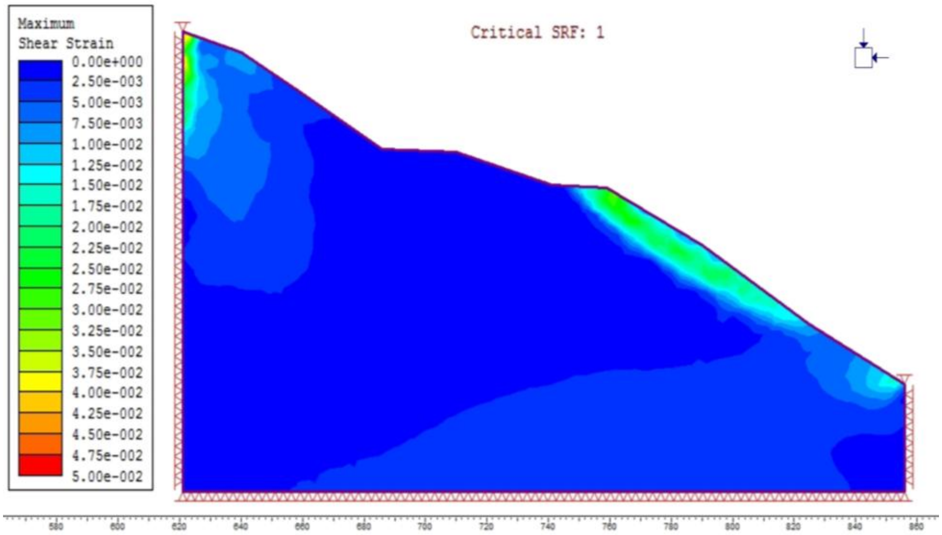
Maximum
Shear Strain
0.00e+000
2.50e-003
5.00e-003
7.50e-003
1.00e-002
1.25e-002
1.50e-002
1.75e-002
2.00e-002
2.25e-002
2.50e-002
2.75e-002
3.00e-002
3.25e-002
3.50e-002
3.75e-002
4.00e-002
4.25e-002
4.50e-002
4.75e-002
5.00e-002
Critical SRF: 1

(a)

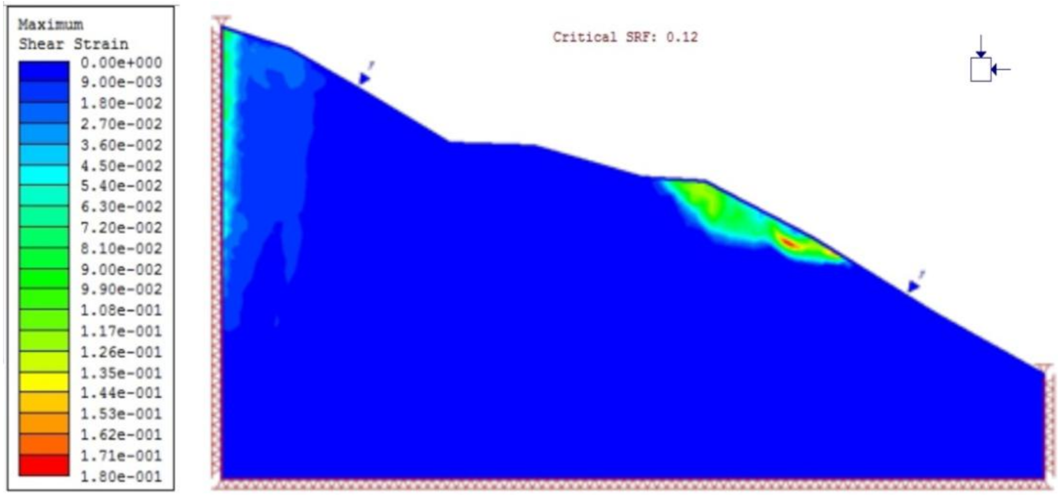
Maximum
Shear Strain
0.00e+000
9.00e-003
1.80e-002
2.70e-002
3.60e-002
4.50e-002
5.40e-002
6.30e-002
7.20e-002
8.10e-002
9.00e-002
9.90e-002
1.08e-001
1.17e-001
1.26e-001
1.35e-001
1.44e-001
1.53e-001
1.62e-001
1.71e-001
1.80e-001
Critical SRF: 0.12

(b)

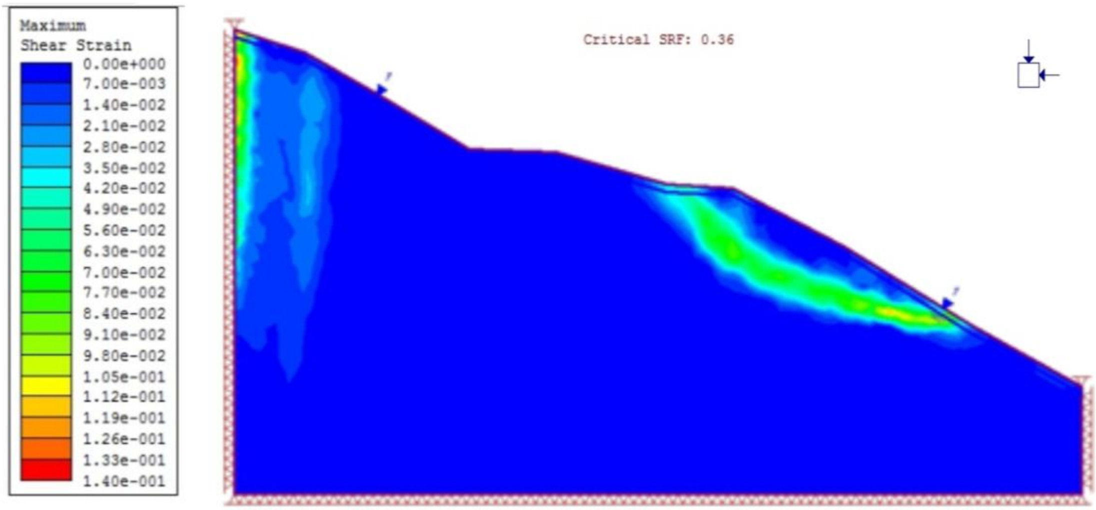
Maximum
Shear Strain
0.00e+000
7.00e-003
1.40e-002
2.10e-002
2.80e-002
3.50e-002
4.20e-002
4.90e-002
5.60e-002
6.30e-002
7.00e-002
7.70e-002
8.40e-002
9.10e-002
9.80e-002
1.05e-001
1.12e-001
1.19e-001
1.26e-001
1.33e-001
1.40e-001
Critical SRF: 0.36

(c)

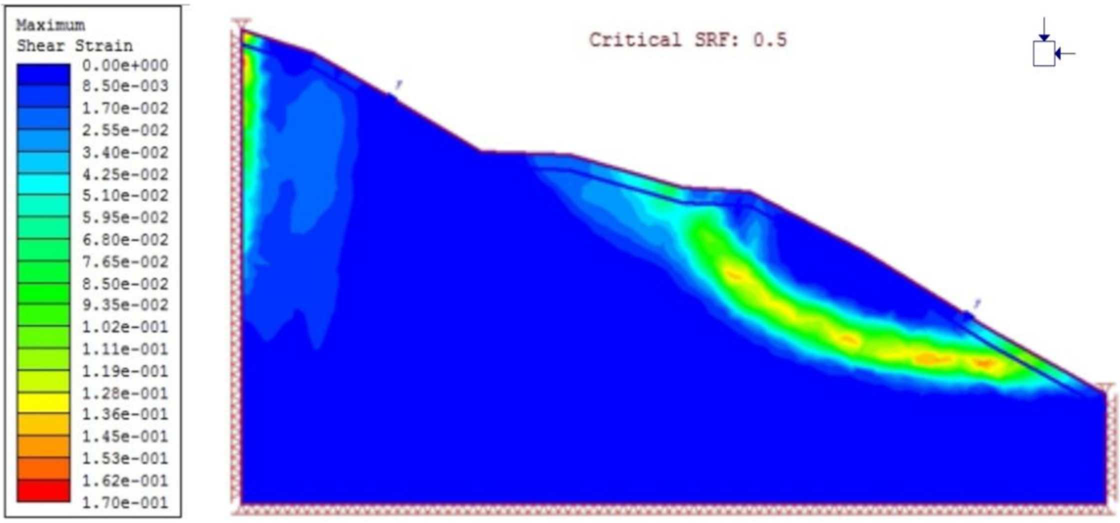

(d)

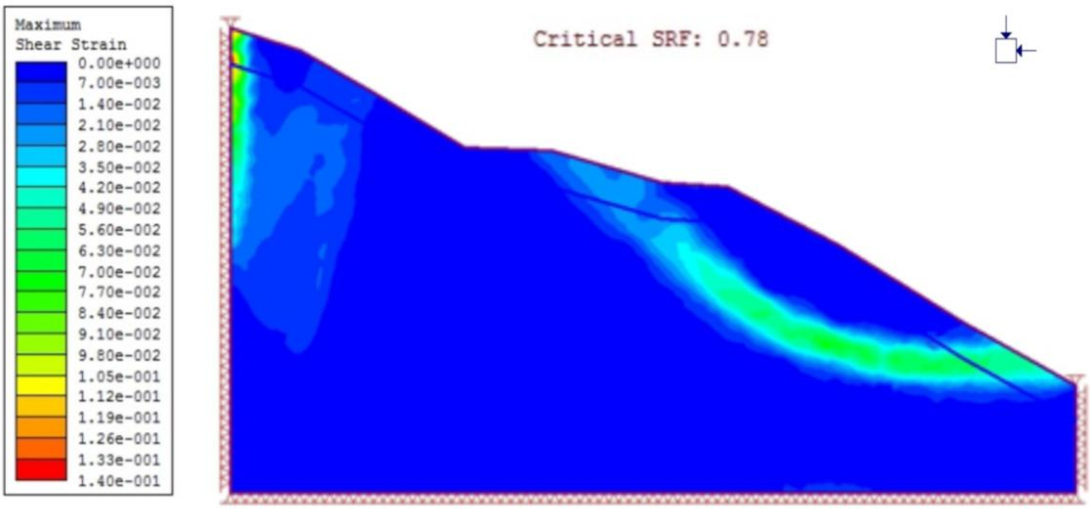

(e)

Figure 13: Maximum shear strain Phase2 result (a) A full dry condition at 1 SRF (b) full saturation condition at 0.12 SRF (c) 2 M GWT down at 0.36 SRF (d) 4 M GWT down at 0.5 SRF (e) 6 M GWT down at 0.78 SRF

3.3 Remedial measures

In the context of the Kuiyadaha creeping failure type of mass movement, two types of remedial measures are proposed: Reduction of Groundwater Table (GWT) and Toe Loading.

In Section One of the Kuiyadaha site, decreasing the groundwater table (GWT) by seven meters resulted in a safety factor one. However, in other parts, simply decreasing the GWT was insufficient to achieve a FOS of 1. Stability investigation revealed that adding toe loading or lifting the toe one to two meters above the initial slope surface increased the FOS value. Table 6 demonstrates that in dry conditions, the stress reduction factor (SRF) exceeds one. The Kuiyadaha slope was subjected to additional stability analysis that combined toe loading with GWT reduction. Table 6 shows the SRF values at various GWT levels, emphasizing the effects of these measures on slope stability.

Table 6: FOS for different condition of Stability measures

Section	S1	S2	S3	S4	S5
Dry condition	1.05	1.13	1.08	1.06	1.03
Saturation condition	0.9	0.2		0.42	0.4
1 m GWT Down					0.5
2 m GWT Down	1	0.4			
3 m GWT Down					0.6
4 m GWT Down	1.1	0.6			
5 m GWT Down				0.66	0.7
6 m GWT Down	1.18	0.7	0.4		
7 m GWT Down					0.8
8 m GWT Down	1.24	0.85			
10 m GWT Down	1.4	0.94	0.53	0.8	0.9
11 m GWT Down		1			
12 m GWT Down					1
14 m GWT Down				0.98	1.1
15 m GWT Down			0.8	1	
16 m GWT Down				1.02	
18 m GWT Down			1		

Table 6 demonstrates that even with toe loading of up to two meters, reaching the appropriate SRF value remains difficult without significantly lowering the groundwater table (GWT). In Section One, the SRF value was obtained with a 2-meter GWT reduction. To reach the targeted stability, Sections Two, Three, Four, and Five required further GWT reductions of 11 meters, 12 meters, 15 meters, and 18 meters, respectively.

4. Conclusions

This study evaluates the slope stability of the Kuiyadaha Landslide using the Back Analysis technique, which has been shown to be extremely useful for analyzing stability conditions. The Kuiyadaha landslide demonstrates creep failure characteristics, with minimal soil movement during the rainy season and stability during the dry season. During the site examination, five soil samples were taken and evaluated for their qualities. The research revealed a friction angle of 30° for Sections One and Two, whereas Sections Three, Four, and Five had friction angles of 26°, 27°, and 28°, respectively. These changes are due to differences in slope gradient and field density between the portions.

The primary tool selected for this research is SPECFEM3D_GEOTECH, which utilizes the Spectral Element Method (SEM), a high-order variant of the Finite Element Method (FEM). Unlike FEM, which uses a generalized mass matrix, SEM employs a diagonalized matrix, resulting in reduced computation time. SPECFEM3D_GEOTECH is a free, open-source, command-driven software designed for 2D and 3D slope stability analysis and for simulating 3D multistage excavations [24]. Stabilization measures included a combination of groundwater table (GWT) reduction and toe loading. Analysis showed that this approach was effective. At section one, a factor of safety (FOS) of 1 was achieved with vertical GWT reductions of 2 meters and in Section Two, three, four and five FOS of 1 were obtained with vertical GWT reductions of 11 meters, 18 meters, 15 meters, and 12 meters, respectively. This research paper focuses on numerical modeling using SEM. To validate the findings, PHASE2 was employed, and a comparison of the results from both tools for section three yielded a correlation value of 0.965, which is considered satisfactory

Conflicts of Interest Statement

The authors declare no conflicts of interest for this study.

Data Availability Statement

The data that support the findings of this study are available from the corresponding author upon reasonable request.

References

1. G. Hancox, "The Abbotsford landslide: its nature and causes," *Thepra: Earth Movements*, 2002, pp. 9–13.
2. J. Remondo, J. Soto, A. González-Díez, J. R. D. de Terán, and A. Cendrero, "Human impact on geomorphic processes and hazards in mountain areas in northern Spain," *Geomorphology*, vol. 66, no. 1–4, pp. 69–84, 2005.
3. G. L. Bennett, S. R. Miller, J. J. Roering, and D. A. Schmidt, "Landslides, threshold slopes, and the survival of relict terrain in the wake of the Mendocino Triple Junction," *Geology*, vol. 44, no. 5, pp. 363–366, 2016.
4. N. Bhandary, R. Tiwari, R. Yatabe, and S. Paudel, "SEM-based seismic slope stability and mitigation model for the Jure landslide after the 7.8 Mw 2015 Barpak-Gorkha, Nepal, earthquake," in *Geotechnical Earthquake Engineering and Soil Dynamics V*, Reston, VA: ASCE, 2018, pp. 88–97.
5. I. Rusydy et al., "Integrated approach in studying rock and soil slope stability in a tropical and active tectonic country," *Environmental Earth Sciences*, vol. 80, pp. 1–20, 2021.
6. S. M. Moreiras, "Climatic effect of ENSO associated with landslide occurrence in the Central Andes, Mendoza Province, Argentina," *Landslides*, vol. 2, pp. 53–59, 2005.
7. J. L. Wong, M. L. Lee, F. Y. Teo, and K. W. Liew, "A review of impacts of climate change on slope stability," in *Climate Change and Water Security: Select Proceedings of VCDRR 2021*, 2021, pp. 157–178.
8. D. N. Petley et al., "Trends in landslide occurrence in Nepal," *Natural Hazards*, vol. 43, pp. 23–44, 2007.
9. M. Jaboyedoff et al., "Human-induced landslides: toward the analysis of anthropogenic changes of the slope environment," in *Landslides and Engineered Slopes: Experience, Theory and Practice*, CRC Press, 2018, pp. 217–232.
10. D. J. Varnes, "Slope movement types and processes," *Special Report*, no. 176, pp. 11–33, 1978.
11. L. Li, Y. Wang, L. Zhang, C. Choi, and C. W. Ng, "Evaluation of critical slip surface in limit equilibrium analysis of slope stability by smoothed particle hydrodynamics," *International Journal of Geomechanics*, vol. 19, no. 5, p. 04019032, 2019.
12. D. Zhu, C. Lee, and H. Jiang, "Generalised framework of limit equilibrium methods for slope stability analysis," *Geotechnique*, vol. 53, no. 4, pp. 377–395, 2003.

13. M. Zolkepli, M. Ishak, and M. Zaini, "Slope stability analysis using modified Fellenius's and Bishop's method," in *IOP Conf. Ser.: Mater. Sci. Eng.*, 2019, IOP Publishing.
14. S. Nasution, S. Rachman, and H. Pramudito, "Slope stability analysis using Bishop method and kinematic analysis," in *IOP Conf. Ser.: Mater. Sci. Eng.*, 2021, IOP Publishing.
15. B. Low and W. H. Tang, "Probabilistic slope analysis using Janbu's generalized procedure of slices," *Computers and Geotechnics*, vol. 21, no. 2, pp. 121–142, 1997.
16. C. Matthews, Z. Farook, and P. Helm, "Slope stability analysis–limit equilibrium or the finite element method," *Ground Engineering*, vol. 48, no. 5, pp. 22–28, 2014.
17. K. P. Aryal, *Slope stability evaluations by limit equilibrium and finite element methods*, 2006.
18. N. A. Hammouri, A. I. H. Malkawi, and M. M. Yamin, "Stability analysis of slopes using the finite element method and limiting equilibrium approach," *Bulletin of Engineering Geology and the Environment*, vol. 67, pp. 471–478, 2008.
19. D. G. Fredlund and R. Scoular, "Using limit equilibrium concepts in finite element slope stability analysis," *Int. Symp. Slope Stability Eng.*, pp. 31–47, 1999.
20. D. Griffiths and P. Lane, "Slope stability analysis by finite elements," *Geotechnique*, vol. 49, no. 3, pp. 387–403, 1999.
21. A. T. Patera, "A spectral element method for fluid dynamics: laminar flow in a channel expansion," *Journal of Computational Physics*, vol. 54, no. 3, pp. 468–488, 1984.
22. R. Tiwari, "Simplified numerical implementation in slope stability modeling," *International Journal of Geomechanics*, vol. 15, no. 3, p. 04014051, 2015.
23. R. C. Tiwari and N. P. Bhandary, "Application of spectral element method (SEM) in slope instability analysis," in *Progress in Landslide Research and Technology, Volume 1 Issue 1*, Springer, 2023, pp. 163–174.
24. H. N. Gharti, D. Komatitsch, V. Oye, R. Martin, and J. Tromp, "Application of an elastoplastic spectral-element method to 3D slope stability analysis," *International Journal for Numerical Methods in Engineering*, vol. 91, no. 1, pp. 1–26, 2012.
25. ASTM D6913, "Standard Test Methods for Particle-Size Distribution (Gradation) of Soils Using Sieve Analysis," ASTM International, West Conshohocken, PA, USA, 2009.
26. ASTM, "Standard Test Method for Particle-Size Distribution (Gradation) of Fine-Grained Soils Using the Sedimentation (Hydrometer) Analysis," 2016.
27. ASTM D4318-10, "Standard test methods for liquid limit, plastic limit, and plasticity index of soils," 2010.
28. R. F. Craig, *Soil Mechanics*, Springer, 2013.
29. B. M. Das and K. Sobhan, *Principles of Geotechnical Engineering*, 1990.
30. J. Zou, H. Chen, Y. Jiang, W. Zhang, and A. Liu, "An effective method for real-time estimation of slope stability with numerical back analysis based on particle swarm optimization," *Applied Rheology*, vol. 33, no. 1, p. 20220143, 2023.
31. I. Brown, P. Wood, and M. Elmouttie, "Estimation of in situ strength from back-analysis of pit slope failure," in *APSSIM 2016: Proc. 1st Asia Pacific Slope Stability in Mining Conf.*, Australian Centre for Geomechanics, 2016.

32. M. Cai et al., "Back-analysis of rock mass strength parameters using AE monitoring data," *Int. J. Rock Mechanics and Mining Sciences*, vol. 44, no. 4, pp. 538–549, 2007.
33. K. You, "A case study on the utilization of tunnel face mapping data for a back analysis based on artificial neural network," *KSCE J. Civil Eng.*, vol. 18, pp. 751–759, 2014.
34. C. Guo et al., "Displacement back analysis of reservoir landslide based on multi-source monitoring data: A case study of the Cheyiping landslide in the Lancang River Basin, China," *Remote Sensing*, vol. 14, no. 11, p. 2683, 2022.
35. J. Mandal, S. Narwal, and S. Gupte, "Back analysis of failed slopes-a case study," *Int. J. Eng. Res. Technol. (IJERT)*, vol. 6, no. 5, 2017.